frontiers | Frontiers in Materials

TYPE Original Research
PUBLISHED 03 November 2023
DOI 10.3389/fmats.2023.1284876

OPEN ACCESS

EDITED BY
Mauro Zarrelli,
National Research Council (CNR), Italy

REVIEWED BY
Atia Atiq,
University of Education Lahore, Pakistan
Yigit Ali Üncü,
Akdeniz University, Türkiye

*CORRESPONDENCE
Seon-Chil Kim,
chil@kmu.ac.kr

RECEIVED 29 August 2023
ACCEPTED 20 October 2023
PUBLISHED 03 November 2023

CITATION
Kim S-C and Youn S (2023), Functional lightweight protective clothing shielding design for constant radiation shielding of flight attendants and Monte Carlo simulation verification.
Front. Mater. 10:1284876.
doi: 10.3389/fmats.2023.1284876

Functional lightweight protective clothing shielding design for constant radiation shielding of flight attendants and Monte Carlo simulation verification

Seon-Chil Kim[1,2]* and Sukwon Youn[3]

[1]Department of Biomedical Engineering, Keimyung University, Daegu, Republic of Korea, [2]Department of Medical Informatics, School of Medicine, Keimyung University, Daegu, Republic of Korea, [3]Department of Applied Bioengineering and Research Institute for Convergence Science, Graduate School of Convergence Science and Technology, Seoul National University, Seoul, Republic of Korea

The use of easily accessible shielding suits for personal defense by flight attendants to reduce occupational cosmic radiation exposure is attracting increasing attention. However, to ensure activity in a limited area, the flexibility of the thin film must be considered. Although several process technologies to reduce the thickness of the shielding fabric are available, nanofiber production through electrospinning is the most effective, and it is attracting attention owing to its excellent reproducibility of the shielding performance. Therefore, in this study, a general sheet and a nanofiber shielding sheet were manufactured, and their shielding performance was compared. In addition, the shielding effect of the nanofiber shielding sheet was verified under aircraft conditions via Monte Carlo simulation. The shielding performance for neutrons and gamma rays, which are the most common sources of cosmic radiation, was 17.5% and 15.2%, respectively, with the Ba-133 and Cs-137 sources in the 0.3 mm shielding fabric. The absorbed dose change with the 5 mm shielding fabric was 7 μGy/d for neutrons and 4.3 μGy/d for protons. The shielding fabric developed in this study is expected to have an active shielding effect when used as personal protective equipment (clothing) by aircrew.

KEYWORDS

air shielding, gadolinium oxide, radiation, radiation shielding, tungsten

1 Introduction

Cosmic radiation is a type of natural radiation that arises from the interaction of high-energy particles entering Earth from inside and outside the solar system with atmospheric particles (Pohl et al., 2020). In general, the average cosmic radiation exposure received on the ground is 0.39 mSv per year because of the reduction in dose by the atmosphere and the shielding effect of Earth's magnetic field (ICNIRP, 2020). However, cosmic radiation exposure increases with altitude, and for crew members who frequently remain at high altitudes during flight, the average annual exposure dose is 1–2 mSv for short-distance flights, which is similar to medical exposure at 3–5 mSv, and approximately 40%–80% of them are estimated to be exposed to neutrons (Zeeb et al., 2012; Yasuda and Yajima, 2018). To ensure user safety, various defense systems are applied in the medical field and other industries that use radiation, considering factors such as shielding, distance, and time.

However, in the aviation industry, no shielding tool has been manufactured or commercialized to protect users from radiation; therefore, the crew is defenselessly exposed (McNeely et al., 2018; Wollschläger et al., 2018; Scheibler et al., 2022). The International Commission on Radiological Protection (ICRP) addresses the occupational exposure of crew members to cosmic radiation during boarding and flight and recommends radiation shielding as the target (Shouop et al., 2020). Although safety management systems related to cosmic radiation exposure are operational in Europe and the United States (Brambilla et al., 2020), the development and dissemination of clear shielding tools remain insufficient, and there is a limit to the development of shields that completely protect sources exposed to neutrons and gamma rays. Furthermore, the shields must satisfy the necessary and sufficient conditions to ensure the smooth functioning of the crew inside the aircraft, considering flexibility in terms of the weight and thickness of the shield. Existing cosmic radiation-shielding materials mainly consist of Kapton-type protective films made of aluminum and polyimide (Peracchi et al., 2021). Aviation shielding can be divided into internal and external shielding. However, personal protective equipment or tools have not been developed thus far (Lee et al., 2020). For personal defense against radiation, personnel in medical institutions typically use an apron with a minimum lead equivalent of 0.25 mm Pb (Adlienė et al., 2020). The internal and external shielding of an aircraft is applied using lead or additional foam made of composite materials. However, the completeness of the shielding may be influenced by the shielding material, composition, and design of the shielding body because the lightweight condition is the most important requirement for the shielding body used in aviation. Therefore, the radiation dose for each flight route is evaluated using codes such as CARI-6, EPCARD, PCAIRE, JISCARD, and SIVERT. These codes, developed to evaluate space radiation exposure doses, are continually validated by airlines and professional research institutes through measurements to ensure accuracy and reliability. In aircraft, it is necessary to develop personal defense products, such as clothing and blankets, that can shield against radiation using lightweight materials that do not interfere with the crew's activities. Therefore, it is necessary to develop lightweight shielding materials that can partially block neutrons and gamma rays. In this study, a flexible sheet or fiber form was considered as a personal defense shielding material, and tungsten (74 W) and gadolinium oxide (Gd_2O_3), which can easily absorb neutrons, were considered as gamma-ray-absorbing materials for the shield (ALMisned et al., 2023; Wang et al., 2023). However, it is difficult to manufacture shields to completely block radiation while ensuring the smooth in-flight activity of flight attendants. Therefore, it is necessary to develop and provide functional materials that reduce radiation through a lightweight shield. Hence, the objective of this study was to fabricate a nanofiber fabric capable of radiation shielding. Lightweight conditions and flexibility were applied to manufacture clothing for flight attendants. The fabrication of radiation shields involves the risk of pinholes, resulting in poor shielding performance (Kuzmin et al., 2021). To solve these problems, nanofiber-based shielding fibers must be fabricated. A sheet form made by mixing existing polymer materials and shielding materials is also possible; however, there is a limit to satisfying the lightweight condition. It is intended to reduce the proportion of polymer materials and obtain a direct defense effect from a material with shielding performance, such as tungsten. Utilizing nanofibers in the manufacture of shields is primarily aimed at achieving lightweight properties. This approach originated with the development of products designed to accommodate user activity, such as those used in medical radiation protection (Kim et al., 2022). To enhance the shielding effect, a layered pattern is applied to evenly distribute the particles of the shielding material, a single sheet of the same thickness is produced, and the shielding performance is compared. The spinning solution used in this study is made into a composite material by mixing polyurethane, tungsten, and gadolinium with a reduced powder particle size, followed by electrospinning (AbuAlRoos et al., 2019). Therefore, a nanofiber fabric with a functional spatial radiation shielding effect rather than complete shielding is developed, and the presence or absence of radiation shielding effects, including gamma rays and neutrons, is verified using a meter and Monte Carlo simulation. If radiation shielding is effective, the manufactured shielding fabric is expected to help reduce individual exposure through products that can be worn by flight attendants at all times.

2 Materials and methods

The performance of cosmic radiation shielding can be improved by increasing the interaction probability between the shielding material and incident radiation (Chancellor et al., 2018). The incident energy intensity attenuated by the interaction between the incident photon and mass per unit area for a specific medium composed of polymer and composite shielding material particles can be calculated using the Beer–Lambert equation, as follows (Mayerhöfer et al., 2020):

$$I = I_{0^{e^{-\mu d}}}, \tag{1}$$

where I_0 represents the incident photon intensity, I represents the transmitted photon intensity, μ (cm^{-1}) is the attenuation factor, and d is the shielding body thickness. The thickness d of the shielding body corresponds to the distance at which the incident ray interacts with the shielding material particles. The mass attenuation coefficient (μ/ρ) of the composite material (where ρ (g/cm^3) represents the density) used in the shielding fabric to be manufactured is the same as that given by Eqs (2), (3) (Hila et al., 2020):

$$\mu/\rho = \frac{1}{\rho d} \mathrm{In}\left(\frac{I_0}{I}\right), \tag{2}$$

$$\mu/\rho = \sum_i w_i \left(\frac{\mu}{\rho}\right)_i. \tag{3}$$

The attenuation of the energy intensity by mass and area directly affects the shielding factor, where $(\mu/\rho)_i$ represents the complex density of the shield, the mass attenuation coefficient of the ith component, and w_i represents the weight fraction. The weight fraction of the ith element in the composite is equal to that obtained from Eq. (4) (Yasmin et al., 2018). Here, a_i and m_i represent the number of decay reactions of the shield mass and the atomic weight of the ith element, respectively.

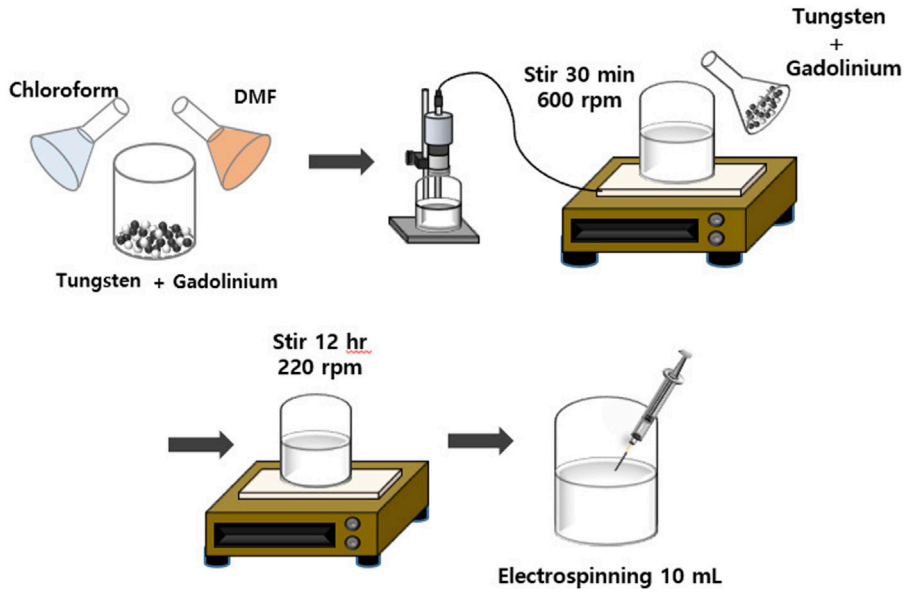

FIGURE 1
Preparation of spinning mixture solution.

$$W_i = \frac{a_i m_i}{\sum_j a_j m_j}. \quad (4)$$

Therefore, the interaction area per unit area should be increased to improve the shielding performance (Evans et al., 2018). In the experiment, a nanofiber-based shielding fabric was fabricated several times to maximize the radiation and interactions between gadolinium oxide and tungsten. It was used to widen the repetitive radiation impact area. The density of gadolinium oxide used for neutron shielding is 7.41 g/cm^3, and the density of the tungsten used for gamma-ray shielding is 19.25 g/cm^3 (Peters et al., 2019; Wicher et al., 2020). Therefore, the mixing ratio of tungsten and gadolinium oxide (purity 99.9%, <4 μm, NanGong XinDun Alloys Spraying Co., Ltd., China) was 7:3 for the composite material. The polymer used for the nanofiber implementation was polyurethane (PU, P-7195A, Mw. = 100,000–150,000, Songwon, Korea). N-dimethylformamide (DMF, 99.5%, Daejung, Korea) was used as the solvent for polymer dissolution. To prepare the mixed spinning solution, as shown in Figure 1, tungsten was placed in a 20-mL glass bottle, and DMF and chloroform were added; then, the mixture was mixed at a speed of 600–800 rpm with a magnetic stirrer (laboratory stirrer/hotplate, PC-420, Corning, Mexico). In addition, when PU was added, the mixing speed was reduced, and the mixture was mixed for ≥12 h to completely dissolve the polymer before spinning.

Using the prepared composite spinning solution, a 0.3 mm nanofiber fabric was manufactured, as shown in Figure 2. The pattern of the nanofiber is affected by the characteristics of the polymer solution, the strength of the electric field, the distance between the nozzle and the collector, and the temperature and humidity (Venkatesan et al., 2020). By adjusting these process parameters and scanning repeatedly, multilayer structure patterns can be obtained. The mixed spinning solution prepared as shown in Figure 2 was first sampled in the same area at regular intervals and time differences. A method of repeating the same type of electrospinning was applied to the prepared shielding area. The electrospray conditions of the mixed spinning solution included a needle size of Gauge 23 or 24 and a voltage of 10 kV. The average distance of the collecting plate was 13–15 cm, the humidity was 25%–40%, and the temperature was 22°C–25°C.

A shielding film in the form of a general shielding sheet was produced, and its shielding performance was compared with that of a sheet made of nanofibers. The fabricated general shielding sheet was prepared by mixing tungsten and gadolinium oxide in a silicone resin (liquid silicone rubber, 100% solid content) at a ratio of 7:3 and stirring at a high speed. For uniform dispersion of the shielding material, high-speed stirring at ≥3,000 rpm was performed, and air defoaming was performed in a vacuum state to form a uniform resin layer (Li et al., 2022). The general sheet was directly coated with the prepared coating resin using the knife over-roll method (gap: 100 μm). It was coated three times (base, main, and top coating) to maximize the amount of application. After coating, each of them was cured at 180 °C for 3 min, and at this time, a general shielding sheet with the same thickness of 0.3 mm was prepared using the necessary silicone curing agent and catalyst. The physical properties of the fabric made of nanofibers are presented in Table 1, and the density was measured as 2.485 g/cm^3. The two prepared shielding fabrics were examined using a field-emission scanning electron microscope (S-4800, Hitachi, Japan) to analyze the internal shielding structure (De Tommasi et al., 2018). In addition, to verify the radiation shielding effect of the two shielding sheets manufactured via different methods using an actual measuring instrument, neutron and gamma-ray shielding experiments were conducted by evaluating Cs-137 and Ba-133. The energy characteristics of Cs-137 (0.01 uCi, half-life 30.2 years, average gamma-ray energy 662 keV) and Ba-133 (1 uCi, half-life 10.6 years, average gamma-ray energy 356 keV) used in the experiment are shown in Figure 3 (Külekçi, 2021).

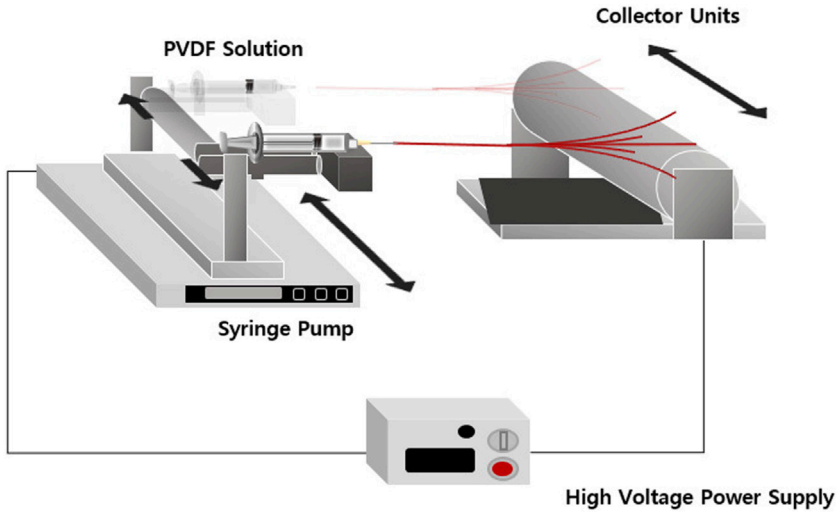

FIGURE 2
Fabrication of nanofibers.

TABLE 1 Physical characteristics of nanofiber fabric.

Weight (kg/m^2)	Tungsten weight (kg/m^2)	Gadolinium oxide weight (kg/m^2)	Thickness (mm)	Density (g/cm^3)
2.041 ± 0.001	0.590 ± 0.001	1.412 ± 0.003	0.300 ± 0.003	2.485 ± 0.000

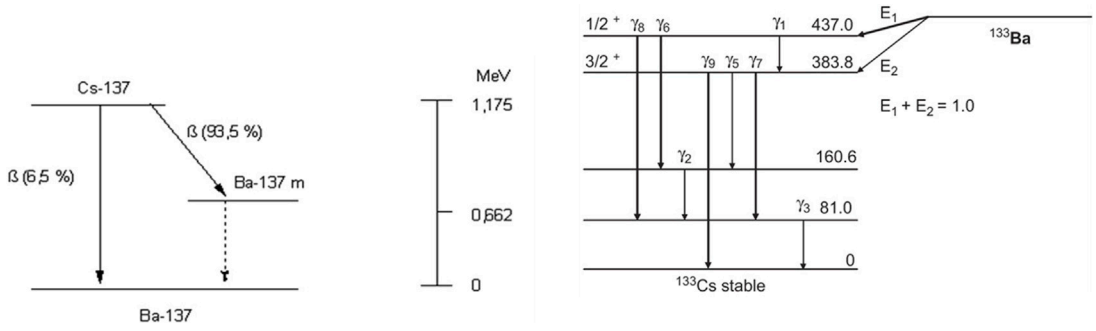

FIGURE 3
Isotope decay diagram of the Cs-137 and Ba-133 sources.

A Mirion DMC 3000 (Mirion Technologies, Inc., Atlanta, United States) was used as the detector for gamma-ray and neutron dose measurements (Abaza, 2018). The correction coefficient for temperature and atmospheric pressure for accurate radiation dose measurement of the detector was confirmed to be 1.0 at a laboratory temperature of 22°C and 1 atm and was used after inspection and calibration. A shielding fabric test was performed, as shown in Figure 4 (Duan et al., 2019). The shielding performance was evaluated according to the pattern model shown in Figure 4. The shielding rate was calculated, as given by Eq. (5), by substituting the case where the manufactured shielding sheet was not discarded and the case where it was discarded.

$$\text{Radiation shielding ratio} = 1 - \left(\frac{D_{NaI}\text{with sheet}}{D_{NaI}\text{without sheet}}\right). \quad (5)$$

Given the difficulty in experimentally verifying the shielding performance against high-energy neutrons and protons inside an actual aircraft, this study employed the MCNP6.2 (Monte Carlo N-Particle version 6.2) particle transport code for secondary verification. The code was used to confirm the shielding effect of neutrons and protons based on the sheild's thickness within the aircraft (Kolacio et al., 2021). As shown in Figure 5, the geometry was constructed, and a Monte Carlo simulation was performed (Hess et al., 1959; Çağlar et al., 2021; Akman et al., 2023). In the case

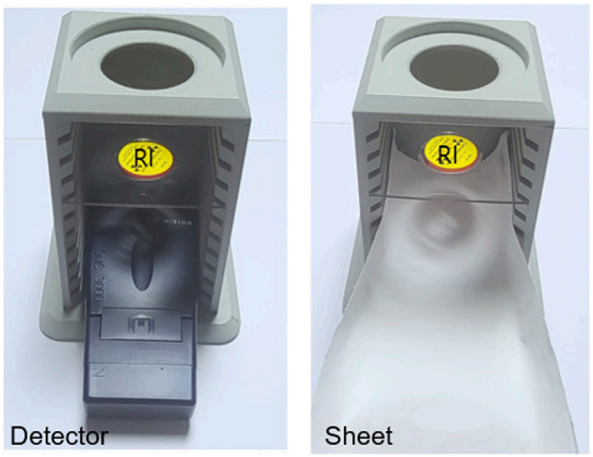

FIGURE 4
Experimental method using the detector.

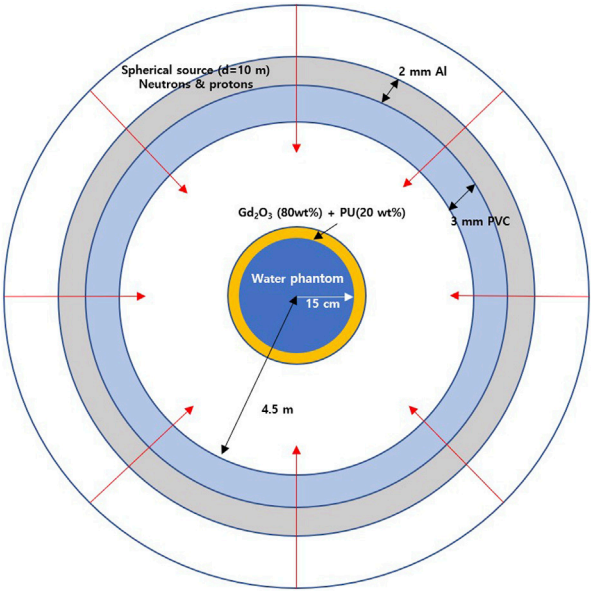

FIGURE 5
Geometry of the Gd_2O_3 + polyurethane sheet in an airplane.

of neutron and proton sources, a spherical surface with a diameter of 10 m was irradiated isotropically from the inside to simulate the shielding effect of the aircraft hull. A spherical shell structure made of polyvinyl chloride (PVC) with a 9 m inner diameter and a 3 mm thickness, coupled with aluminum of 2 mm thickness, was designed inside the source. At the center, a spherical water phantom with a 30 cm diameter was wrapped with a spherical shell-shaped shielding material made of gadolinium oxide (Gd_2O_3) and polyurethane (PUR) to evaluate the shielding effect.

The shielding body consisted of 80 wt% Gd_2O_3 and 20 wt% PUR. The study assessed the absorbed 1-day dose of high-energy neutrons and protons at the aircraft's altitude for a water phantom with a 30 cm inner diameter, both without a shield and with shield

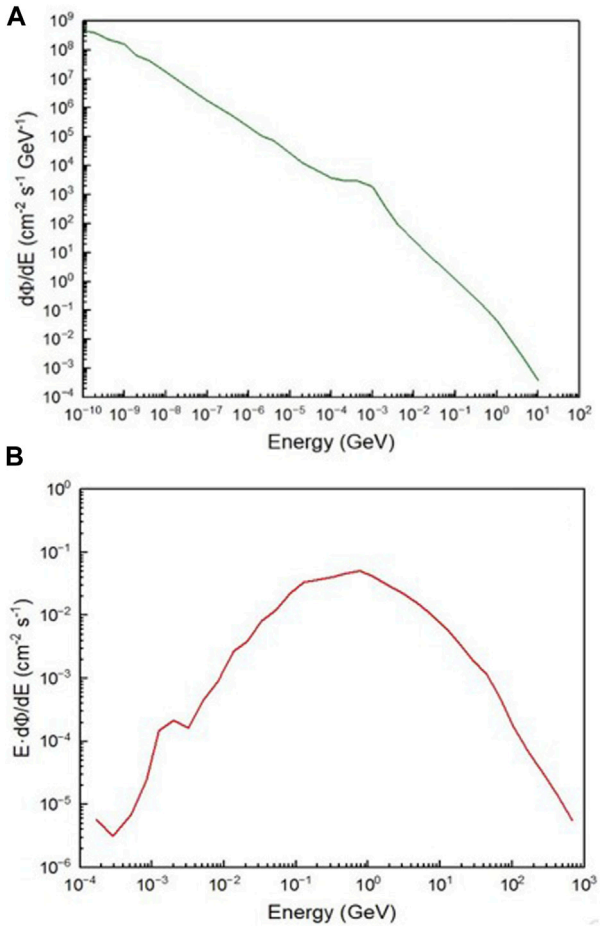

FIGURE 6
Aircraft altitude neutron spectrum **(A)** and proton spectrum **(B)**.

thicknesses of 2.5, 5, 10, 15, 20, and 25 mm, using the F6 tally. For aircraft altitude neutron sources, the study used the neutron spectrum measured at 200 g/cm^2 atmospheric depth (altitude 11.9 km) by Hess et al., as shown in Figure 6. For the proton source, the spectrum obtained through Roesler et al.'s FLUKA simulation at a 200 g/cm^2 atmospheric depth was used, as shown in Figure 6 (200 g/cm^2 corresponds to an altitude of 11.9 km) (Roesler et al., 1998; Zieb et al., 2018). The particle histories used were 10^9 for neutrons and 10^8 for protons.

3 Results

The shielding fabric implemented by electrospinning using a spinning solution mixed with tungsten and gadolinium oxide is shown in Figure 7A. It had a slightly grayish appearance because of the tungsten, and the thickness was 0.3 ± 0.002 mm. As shown in Figure 7B, the shielding sheet had a thickness of 0.3 ± 0.05 mm. The prototype was 500 mm in length and width and was manufactured to a size that covered the detector.

Figure 8 shows an enlarged image of the cross section of the shielding fabric, and Figure 9 shows a cross-sectional image of the shielding sheet produced by the general process. Each cross-sectional

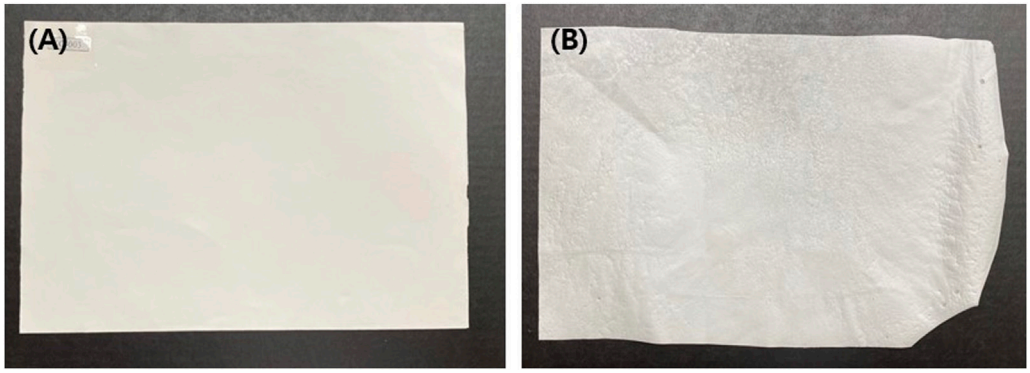

FIGURE 7
Electrospinning process for the shielding sheet **(A)** and general process of shielding **(B)** according to manufacturing method.

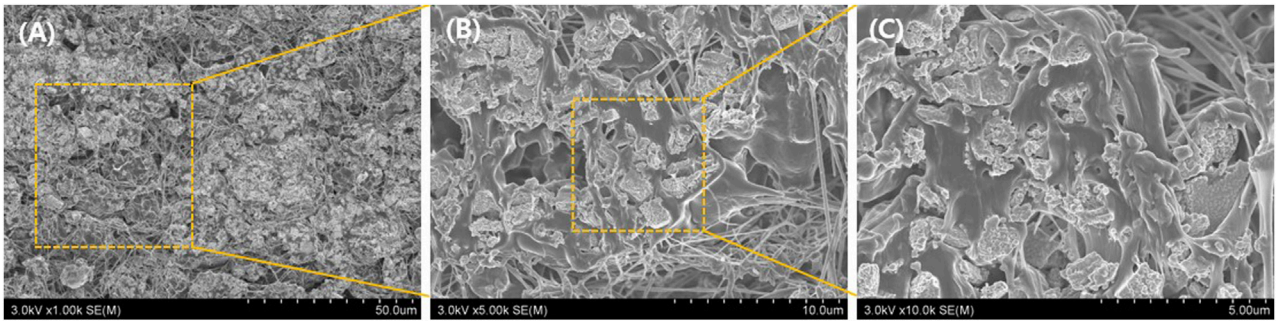

FIGURE 8
Electron microscopic cross-sectional image of nano-shielding fibers in the electrospinning process; the dispersion state of the shielding material was checked by expanding to **(A)**, **(B)**, and **(C)**.

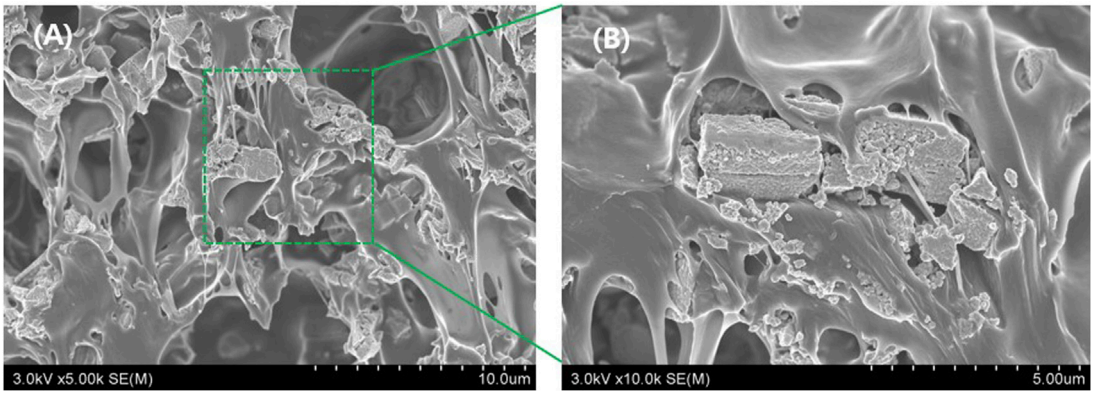

FIGURE 9
Cross-sectional image of the shielding sheet under electron microscopy in the general process; the dispersion state of the shielding material was confirmed by expanding to **(A)** and **(B)**.

image was enlarged to visually confirm the dispersion state of the shielding material according to the nanofiber and general sheet shape. The cross-sectional image confirmed that the particle dispersion shape of the shielding material depended on the distribution state of the polymer material. When the particle distribution was enlarged and compared, as shown in Figure 8A, it was found that the distribution of the fibrous particles was better dispersed, and the spacing between the tungsten and gadolinium particles was well-controlled. In the internal structure of the shielding sheet shown in Figure 9A, the dispersion was slightly insufficient owing to the aggregation of polymers.

TABLE 2 Shielding rate evaluation of Ba-133 and Cs-137.

Shield	Ba-133		Cs-137	
	Dose rate (uSv/h)	Shielding rate (%)	Dose rate (uSv/h)	Shielding rate (%)
Nanofiber fabric	5.72	17.5 ± 2.4	6.09	12.2 ± 3.4
Shielding sheet	1.16	15.2 ± 1.2	1.49	10.2 ± 1.8

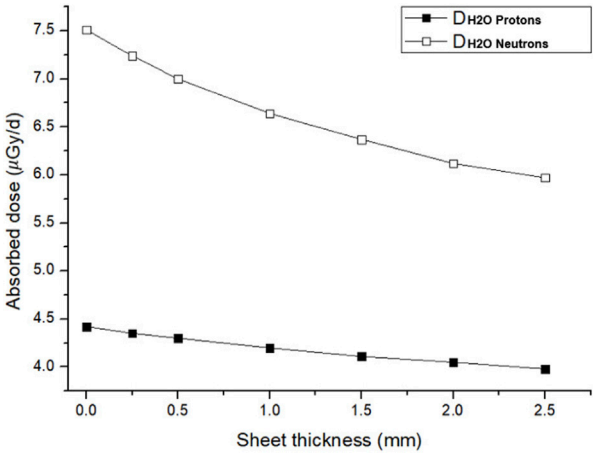

FIGURE 10
Change rate of the absorbed dose due to cosmic radiation at aircraft altitude according to the thickness of the shielding sheet.

For a full-time shielding suit for aircrew, the shielding performance was verified using two sources: Ba-133 and Cs-137. As shown in Table 2, the shielding rates were generally similar, but those of the fabrics made of nanofibers were higher. The shielding ratio was between 12.2% and 17.5% for fibers and between 10.2% and 15.2% for sheets.

As shown in Figure 10, the change in the absorbed dose during the day was confirmed when there was no shielding sheet and when the thickness of the sheet was 2, 5, 5, 10, 15, 20, and 25 mm, for a water phantom with a diameter of 30 cm inside the sheet. For both neutrons and protons, the shielding effect increased with the thickness, and the shielding efficiency was higher for protons than for neutrons.

4 Discussion

Appropriate measures are needed to protect the crew and passengers of aircraft operating on the Northern Sea Route from cosmic radiation (Jang et al., 2011). Efforts to achieve complete defense are necessary; however, it is important to develop safe shielding materials that do not impair their activities. Nuclear industry and radiation medical workers are exposed to 1.87 and 0.75 mSv, respectively, whereas aircraft crew members are reported to have an annual exposure of 3.07 mSv (Seo et al., 2018). Therefore, securing the management and safety standards for cumulative exposure to cosmic radiation is an urgent task. This paper proposes a system capable of shielding at a level that can be worn by flight attendants at all times, for which a shielding fabric was developed. Analyzing the source at 2 uSv/h of cosmic radiation revealed that neutrons account for approximately 0.7 uSv/h, protons and gamma rays account for 0.3 uSv/h each, and electron beams account for approximately 0.2 uSv/h (Norbury et al., 2019; Shavers et al., 2023). Owing to the large proportion of neutrons, complete interception in practice can present a difficult environment for flight attendants and passengers. Approximately 20% shielding performance can be obtained with a thickness of <0.4 mm; therefore, it is considered that daily work that does not receive many suggestions for the amount of activity in the aircraft is possible. Therefore, if the shielding of the aircraft itself and a multilevel shielding system through clothing are realized, a satisfactory level of shielding can be achieved. As demonstrated in the experiment, the performance of 0.3 mm shielding fabric was 15%, and more effective shielding can be expected in the case of a multilayer structure. The shielding nanofiber fabric realized via electrospinning can safely reproduce the shielding performance, and the mixing area of the shielding material is free. In particular, it can be flexibly implemented in a desired shape; therefore, personal protective equipment such as blankets and clothing can be developed for flight attendants and passengers. Currently, the shape produced in the laboratory is implemented through one nozzle; however, the mass production of air shields can be realized by spraying the spinning solution using a large number of syringes. However, the specific gravity of the tungsten used in this experiment is large in the nozzle and collection distance; therefore, it is necessary to adjust the distance per hour. Temperature and humidity in the electric field are also influencing factors (Li et al., 2020). Combining these process variables can allow the mass production of shielding fabrics while maintaining the reproducibility of the shielding performance. Exposure to aerospace radiation involves low-dose radiation of ≤6 mSv; however, considering continuous exposure during working hours, wearing it at all times can be recognized as the most effective countermeasure (Bramlitt, 2018). The limitations of this study are that the shielding performance was evaluated using neutron and gamma-ray sources rather than a shielding experiment using actual cosmic radiation, and the change in the absorbed dose trended through the simulation (Hu et al., 2020). To achieve shielding from cosmic radiation, cabin design changes, flight route modifications, and personal protective equipment can be considered. Furthermore, the most economical protection method is the use of personal protective equipment, e.g., clothing and blankets, which are effective (Dogan et al., 2019). Our study is constrained by the utilization of two radiation sources, Ba-133 and Cs-137, for space radiation experiments abundant in neutrons. Given the dose rate's variability depending on the space environment, we aim to correlate it with an approximation of the actual measured value. A functional radiation protection product can be developed in the form of a shielding sheet; however, in the case of the sheet, the particle control of the shielding material is irregularly performed, similar to the case of this study. When the shielding material

is fabricated with nanofibers, the particles can be effectively dispersed, which is beneficial for reproducibility. For aerospace radiation, the conditional theory of harm is still applied, and there are cases in which the exposure of aircrew to radiation is ignored at low doses (Meier et al., 2020). However, as the exact risk dose has not yet been determined, the crew and passengers of the aircraft must be protected. The development of such personal protective equipment should be continued, and many tools are expected to be developed on the basis of these studies.

5 Conclusion

To shield against aerospace radiation, a shielding fabric with a personal defense function for a crew member was developed and manufactured. Measurement of the absorbed dose using a 5 mm shielding fabric resulted in Monte Carlo simulation results of 7 μGy/d for neutrons and 4.3 μGy/d for protons. The shielding fabric made of 0.3 mm nanofibers exhibited shielding rates of 17.5% for Ba-133% and 15.2% for Cs-137. Furthermore, the fabric woven with nanofibers had a higher shielding rate (by ≥ 2%) than the general sheet. Therefore, the nanofiber shielding fabric with increased flexibility achieved by reducing the thickness can be used by flight attendants as a personal defense tool for active cosmic radiation protection during flight.

Data availability statement

The original contributions presented in the study are included in the article/Supplementary Material, further inquiries can be directed to the corresponding author.

Author contributions

S-CK: Conceptualization, Formal Analysis, Funding acquisition, Project administration, Supervision, Writing–original draft, Writing–review and editing. SY: Funding acquisition, Methodology, Software, Supervision, Writing–review and editing.

Funding

The author(s) declare financial support was received for the research, authorship, and/or publication of this article. This work was supported by the Radiation Technology R&D program through the National Research Foundation of Korea, funded by the Ministry of Science and ICT (2020M2C8A1056950).

Conflict of interest

The authors declare that the research was conducted in the absence of any commercial or financial relationships that could be construed as a potential conflict of interest.

Publisher's note

All claims expressed in this article are solely those of the authors and do not necessarily represent those of their affiliated organizations, or those of the publisher, the editors and the reviewers. Any product that may be evaluated in this article, or claim that may be made by its manufacturer, is not guaranteed or endorsed by the publisher.

References

Abaza, A. M. H. (2018). New trend in radiation dosimeters. *Am. J. Mod. Phys.* 7 (1), 21–30. doi:10.11648/j.ajmp.20180701.13

AbuAlRoos, N. J., Amin, N. A. B., and Zainon, R. (2019). Conventional and new lead-free radiation shielding materials for radiation protection in nuclear medicine: a review. *Radiat. Phys. Chem.* 165, 108439. doi:10.1016/j.radphyschem.2019.108439

Adlienė, D., Gilys, L., and Griškonis, E. (2020). Development and characterization of new tungsten and tantalum containing composites for radiation shielding in medicine. *Nucl. Instrum. Methods Phys. Res. B Beam Interact. Mater. At.* 467, 21–26. doi:10.1016/j.nimb.2020.01.027

Akman, F., Ozdogan, H., Kilicoglu, O., Ogul, H., Agar, O., Kacal, M. R., et al. (2023). Gamma, charged particle and neutron radiation shielding capacities of ternary composites having polyester/barite/tungsten boride. *Radiat. Phys. Chem.* 212, 111120. doi:10.1016/j.radphyschem.2023.111120

Almisned, G., Baykal, D. S., Ali, F. T., Bilal, G., Kilic, G., and Tekin, H. O. (2023). Gadolinium-tungsten-boron trioxide glasses: a multi-phase research on cross-sections, attenuation coefficients, build-up factors and individual transmission factors using MCNPX. *Optik* 272, 170216. doi:10.1016/j.ijleo.2022.170216

Bagshaw, M., and Illig, P. (2019). *Travel medicine*. Amsterdam: Elsevier.

Brambilla, M., Vassileva, J., Kuchcinska, A., and Rehani, M. M. (2020). Multinational data on cumulative radiation exposure of patients from recurrent radiological procedures: call for action. *Eur. Radiol.* 30, 2493–2501. doi:10.1007/s00330-019-06528-7

Bramlitt, E. T. (2018). NIST-traceable neutron dosimetry is needed for air travel radiation safety. *Health Phys.* 114 (4), 460. doi:10.1097/HP.0000000000000829

Çağlar, M., Karabul, Y., Kılıç, M., Özdemir, Z. G., and İçelli, O. (2021). Na2Si3O7/Ag micro and nano-structured glassy composites: the experimental and MCNP simulation surveys of their radiation shielding performances. *Prog. Nucl. Energy* 139, 103855. doi:10.1016/j.pnucene.2021.103855

Chancellor, J. C., Blue, R. S., Cengel, K. A., Auñón-Chancellor, S. M., Rubins, K. H., Katzgraber, H. G., et al. (2018). Limitations in predicting the space radiation health risk for exploration astronauts. *NPJ Microgravity* 4, 8. doi:10.1038/s41526-018-0043-2

De Tommasi, E., Congestri, R., Dardano, P., De Luca, A. C., Managò, S., Rea, I., et al. (2018). UV-shielding and wavelength conversion by centric diatom nanopatterned frustules. *Sci. Rep.* 8, 16285. doi:10.1038/s41598-018-34651-w

Dogan, S., Kayacan, O., and Goren, A. (2019). A lightweight, strength and electromagnetic shielding polymer composite structure for infant carrier strollers. *Polym. Compos.* 40 (12), 4559–4572. doi:10.1002/pc.25324

Duan, J., Wang, X., Li, Y., and Liu, Z. (2019). Effect of double-layer composite absorbing coating on shielding effectiveness of electromagnetic shielding fabric. *Mater. Res. Express* 6 (8), 086109. doi:10.1088/2053-1591/ab1d2d

Evans, B. R., Lian, J., and Ji, W. (2018). Evaluation of shielding performance for newly developed composite materials. *Ann. Nucl. Energy* 116, 1–9. doi:10.1016/j.anucene.2018.01.022

Hess, W. N., Patterson, H. W., Wallace, R., and Chupp, E. L. (1959). Cosmic-ray neutron energy spectrum. *Phys. Rev.* 116 (2), 445–457. doi:10.1103/PhysRev.116.445

Hila, F. C., Amorsolo, A. V., Javier-Hila, A. M. V., and Guillermo, N. R. D. (2020). A simple spreadsheet program for calculating mass attenuation coefficients and shielding parameters based on EPICS2017 and EPDL97 photoatomic libraries. *Radiat. Phys. Chem.* 177, 109122. doi:10.1016/j.radphyschem.2020.109122

Hu, G., Hu, H., Yang, Q., Yu, B., and Sun, W. (2020). Study on the design and experimental verification of multilayer radiation shield against mixed neutrons and γ-rays. *Nucl. Eng. Technol.* 52 (1), 178–184. doi:10.1016/j.net.2019.07.016

International Commission on Non-Ionizing Radiation Protection (ICNIRP) (2020). Principles for non-ionizing radiation protection. *Health Phys.* 118, 477–482.

Jang, T. S., Oh, D. S., Kim, J. K., Kang, K. I., Cha, W. H., and Rhee, S. W. (2011). Development of multi-functional composite structures with embedded electronics for

space application. *Acta Astronaut.* 68 (1–2), 240–252. doi:10.1016/j.actaastro.2010.08.009

Kaynan, O., Atescan, Y., Ozden-Yenigun, E., and Cebeci, H. (2018). Mixed mode delamination in carbon nanotube/nanofiber interlayered composites. *Compos. B Eng.* 154, 186–194. doi:10.1016/j.compositesb.2018.07.032

Kim, S. C., and Byun, H. (2022). Development of ultra-thin radiation-shielding paper through nanofiber modeling of morpho butterfly wing structure. *Sci. Rep.* 12, 22532. doi:10.1038/s41598-022-27174-y

Kolacio, M. S., Brkić, H., Faj, D., Radojčić, D. S., Rajlić, D., Obajdin, N., et al. (2021). Validation of two calculation options built in Elekta Monaco Monte Carlo based algorithm using MCNP code. *Radiat. Phys. Chem.* 179, 109237. doi:10.1016/j.radphyschem.2020.109237

Külekçi, G. (2021). Investigation of fly ash added light concretes with respect to gamma radiation transmission properties of ^{133}Ba and ^{137}Cs. *Radiat. Eff. Defects Solids* 176 (9–10), 833–844. doi:10.1080/10420150.2021.1963726

Kuzmin, A. A., Khazanov, E. A. E., and Shaykin, A. A. (2021). Pulse energy limitation of high-power nanosecond lasers due to plasma generation in spatial filters. *Journal of Electron Optics* 51, 142. doi:10.1070/QEL17452

Lee, J. H., Kim, H. N., Jeong, H. Y., and Cho, S. O. (2020). Optimization of shielding to reduce cosmic radiation damage to packaged semiconductors during air transport using Monte Carlo simulation. *Nucl. Eng. Technol.* 52 (8), 1817–1825. doi:10.1016/j.net.2020.01.016

Li, J., Liu, X., Sun, H., Wang, L., Zhang, J., Deng, L., et al. (2020). An optical fiber sensor coated with electrospinning polyvinyl alcohol/carbon nanotubes composite film. *Sensors* 20 (23), 6996. doi:10.3390/s20236996

Li, M., Cao, B., Liu, Y., and Wang, L. (2022). Novel microcapsule-doped insulating materials with hydrophobic transfer ability triggered by creepage discharge. *High Voltage* 7, 950–959. doi:10.1049/hve2.12193

Mayerhöfer, T. G., Pahlow, S., and Popp, J. (2020). The Bouguer-Beer-Lambert law: Shining light on the obscure. *ChemPhysChem* 21 (18), 2029–2046. doi:10.1002/cphc.202000464

McNeely, E., Mordukhovich, I., Staffa, S., Tideman, S., Gale, S., and Coull, B. (2018). Cancer prevalence among flight attendants compared to the general population. *Environ. Health* 17, 49. doi:10.1186/s12940-018-03968

Meier, M. M., Copeland, K., Klöble, K. E. J., Matthiä, D., Plettenberg, M. C., Schennetten, K., et al. (2020). Radiation in the atmosphere—a hazard to aviation safety? *Atmosphere* 11 (12), 1358. doi:10.3390/atmos11121358

Naito, M., Hasebe, N., Shikishima, M., Amano, Y., Haruyama, J., Matias-Lopes, J. A., et al. (2020). Radiation dose and its protection in the Moon from galactic cosmic rays and solar energetic particles: at the lunar surface and in a lava tube. *J. Radiol. Prot.* 40 (4), 947–961. doi:10.1088/1361-6498/abb120

Norbury, J. W., Slaba, T. C., Aghara, S., Badavi, F. F., Blattnig, S. R., Clowdsley, M. S., et al. (2019). Advances in space radiation physics and transport at NASA. *Life Sci. Space Res.* 22, 98–124. doi:10.1016/j.lssr.2019.07.003

Peracchi, S., James, B., Pagani, F., Pan, V., Vohradsky, J., Bolst, D., et al. (2021). Radiation shielding evaluation of spacecraft walls against heavy ions using microdosimetry. *IEEE Trans. Nucl. Sci.* 68 (5), 897–905. doi:10.1109/TNS.2020.3032946

Peters, R., Beiss, P., and Lindlohr, S. (2019). Density determination of sintered steel – results of a round robin test: Dedicated to Stefan Lindlohr who had to leave us much too early. *Pract. Metallogr.* 56 (11), 731–746. doi:10.3139/147.110614

Pohl, M., Hoshino, M., and Niemiec, J. (2020). PIC simulation methods for cosmic radiation and plasma instabilities. *Prog. Part. Nucl. Phys.* 111, 103751. doi:10.1016/j.ppnp.2019.103751

Roesler, S., Heinrich, W., and Schraube, H. (1998). Calculation of radiation fields in the atmosphere and comparison to experimental data. *Radiat. Res.* 149 (1), 87–97. doi:10.2307/3579685

Scheibler, C., Toprani, S. M., Mordukhovich, I., Schaefer, M., Staffa, S., Nagel, Z. D., et al. (2022). Cancer risks from cosmic radiation exposure in flight: a review. *Front. Public Health* 10, 947068. doi:10.3389/fpubh.2022.947068

Seo, S., Lim, W. Y., Lee, D. N., Kim, J. U., Cha, E. S., Bang, Y. J., et al. (2018). Assessing the health effects associated with occupational radiation exposure in Korean radiation workers: protocol for a prospective cohort study. *BMJ Open* 8, e017359. doi:10.1136/bmjopen-2017-017359

Shavers, M., Semones, E., Tomi, L., Chen, J., Straube, U., Komiyama, T., et al. (2023). Space agency-specific standards for crew dose and risk assessment of ionising radiation exposures for the International Space Station. *Z. fur Med. Phys.* doi:10.1016/j.zemedi.2023.06.005

Shouop, C. J. G., Moyo, M. N., Mekongtso, E. J. N., Cho, K., and Strivay, D. (2020). Radiological protection requirements with regard to cosmic ray exposure during air travel. *Eur. Phys. J. Plus* 135 (5), 438. doi:10.1140/epjp/s13360-020-00468-8

Venkatesan, M., Veeramuthu, L., Liang, F.-C., Chen, W.-C., Cho, C.-J., Chen, C.-W., et al. (2020). Evolution of electrospun nanofibers fluorescent and colorimetric sensors for environmental toxicants, pH, temperature, and cancer cells – a review with insights on applications. *Chem. Eng. J.* 397, 125431. doi:10.1016/j.cej.2020.125431

Wang, K., Ma, L., Yang, C., Bian, Z., Zhang, D., Cui, S., et al. (2023). Recent progress in Gd-containing materials for neutron shielding applications: a review. *Materials* 16 (12), 4305. doi:10.3390/ma16124305

Wicher, B., Zdunek, K., Chodun, R., Haj Ibrahim, S., Kubiś, M., Lachowski, A., et al. (2020). Surface sintering of tungsten powder targets designed by electromagnetic discharge: a novel approach for film synthesis in magnetron sputtering. *Mater. Des.* 191, 108634. doi:10.1016/j.matdes.2020.108634

Wollschläger, D., Hammer, G., Schafft, T. T., Dreger, S., Blettner, M., and Zeeb, H. (2018). Estimated radiation exposure of German commercial airline cabin crew in the years 1960–2003 modeled using dose registry data for 2004–2015. *J. Expo. Sci. Environ. Epidemiol.* 28, 275–280. doi:10.1038/jes.2017.21

Yasmin, S., Barua, B. S., Khandaker, M. U., Chowdhury, F.-U.-Z., Rashid, A., Bradley, D. A., et al. (2018). Studies of ionizing radiation shielding effectiveness of silica-based commercial glasses used in Bangladeshi dwellings. *Results Phys.* 9, 541–549. doi:10.1016/j.rinp.2018.02.075

Yasuda, H., and Yajima, K. (2018). Verification of cosmic neutron doses in long-haul flights from Japan. *Radiat. Meas.* 119, 1350–4487. doi:10.1016/j.radmeas.2018.08.016

Zeeb, H., Hammer, G. P., and Blettner, M. (2012). Epidemiological investigations of aircrew: an occupational group with low-level cosmic radiation exposure. *J. Radiol. Prot.* 32 (1), N15–N19. doi:10.1088/0952-4746/32/1/N15

Zieb, K., Hughes, H. G., James, M. R., and Xu, X. G. (2018). Review of heavy charged particle transport in MCNP6.2. *Nucl. Instrum. Methods. Phys. Res. B* 886, 77–87. doi:10.1016/j.nima.2018.01.002